Original Article

MARINE BIOTECHNOLOGY

A Novel Matrix Protein p10 from the Nacre of Pearl Oyster (*Pinctada fucata*) and Its Effects on Both $CaCO_3$ Crystal Formation and Mineralogenic Cells

Cen Zhang,[1] Shuo Li,[1] Zhuojun Ma,[1] Liping Xie,[1,2] Rongqing Zhang[1,2]

[1]Institute of Marine Biotechnology, Department of Biological Sciences and Biotechnology, Tsinghua University, Beijing 100084, People's Republic of China
[2]Protein Science Laboratory of the Ministry of Education, Tsinghua University, Beijing 100084, People's Republic of China

Received: 9 March 2006 / Accepted: 29 April 2006 / Published online: 18 September 2006

Abstract

A novel matrix protein, designated as p10 because of its apparent molecular mass of 10 kDa, was isolated from the nacreous layer of pearl oyster (*Pinctada fucata*) by reverse-phase high-performance liquid chromatography. In vitro crystallization experiments showed that p10 could accelerate the nucleation of calcium carbonate crystals and induce aragonite formation, suggesting that it might play a key role in nacre biomineralization. As nacre is known to contain osteogenic factors, two mineralogenic cell lines, MRC-5 fibroblasts and MC3T3-E1 preosteoblasts, were used to investigate the biological activity of p10. The results showed that p10 could increase alkaline phosphatase activity, an early marker of osteoblast differentiation, while the viability of MRC-5 and MC3T3-E1 remained unchanged after treatment of p10. Taken together, the findings led to identification of a novel matrix protein from the nacre of *P. fucata* that plays a role in both the mineral phase and in the differentiation of the cells involved in biomineralization.

Keywords: Aragonite — biomineralization — bone formation — nacre — soluble matrix proteins

Introduction

In recent years, the nacre (also called mother-of-pearl) of molluscs has drawn much attention for its extraordinary mechanical properties and osteogenic capability (Westbroek and Marin, 1998; Kamat et al., 2000; Rubner, 2003; Zhang and Zhang, 2006). Nacre consists of more than 95% calcium carbonate deposited as aragonite and about 5% of organic matrix. Although accounting for only less than 5% in nacre weight, the organic matrix proteins is thought to direct the formation of the calcium carbonate crystals and in this way contributes to the extraordinary properties of the nacre.

Purification and functional characterization of these organic matrix proteins are helpful to understand the molecular mechanisms of nacre formation. So far, several matrix proteins have been identified from the nacre of pearl oyster *Pinctada fucata* and other molluscs, and their distributions and functions in controlling calcium carbonate crystal formation have also been extensively investigated (Samata et al., 1999; Kono et al., 2000; Marin et al., 2000; Weiss et al., 2000, 2001; Zhang et al., 2003; Jolly et al., 2004; Fu et al., 2005; Takeuchi and Endo, 2006; Zhang and Zhang, 2006). These matrix proteins were generally extracted via a decalcification process involving ethylenediaminetetraacetic acid (EDTA) or weak acid (usually acetic acid), and thus were classified as soluble matrix proteins or insoluble matrix proteins according to their solubility in this process (Samata et al., 1999; Kono et al., 2000; Marin et al., 2000; Weiss et al., 2000, 2001; Fu et al., 2005; Zhang and Zhang, 2006). However, because nacre formation is a complex process involving multiple matrix proteins, some unknown matrix proteins may also play important roles in this process.

Recently, it was found that the nacre of *Pinctada maxima* had osteogenic effects in in vitro and in vivo experiments (Lopez et al., 1992, 2004; Silve et al., 1992; Atlan et al., 1999; Lamghari et al.,2001),

Correspondence to: Liping Xie and Rongqing Zhang; E-mail: lpxie@mail.tsinghua.edu.cn and rzhang@mail.tsinghua.edu.cn

 DOI: 10.1007/s10126-006-6037-1 • Volume 8, 624–633 (2006)

and further investigation showed that the soluble matrix extracted by water could act on proliferation and differentiation of bone-related cells such as fibroblasts and osteoblasts (Lamghari et al., 1999; Almeida et al., 2000, 2001; Moutahir-Belqasmi et al., 2001; Pereira-Mouries et al., 2002a; Rousseau et al., 2003; Lopez et al., 2004). Analysis of this soluble matrix extracted by water showed that it is quite different from that extracted with EDTA. The soluble matrix extracted by water without decalcification is hydrophobic, and the main protein fraction has silk-like properties, while the soluble matrix extracted with decalcification by EDTA is by and large very hydrophilic (Pereira-Mouries et al., 2002b). These suggested that a small portion of the nacre organic matrix containing osteogenic signal molecules can be extracted without dissolving the minerals. However, until now no matrix protein with osteogenic properties in this extract has been reported.

In the present study, using an undecalcification extraction with phosphate buffer (pH 7.0), a new soluble matrix protein was purified from the nacre extract of *Pinctada fucata*, the functions of which in nacre biomineralization and effects on mammalian cells were investigated.

Materials and Methods

Protein Extraction and Purification of p10. The shell of *P. fucata* was obtained from Guofa Pearl Farm (Beihai, Guangxi Province, China). The nacre was mechanically separated from the clean crushed shell and then powdered. Powdered nacre (100 g) was suspended in 500 ml of 2 mM Na_2HPO_4-KH_2PO_4 buffer (pH 7.0) for 3 days at 4°C with continuous stirring. The suspension was then centrifuged at 12,000 rpm for 30 min at 4°C. The supernatant solution was concentrated by ultrafiltration with an 8050 Amicon stirred cell (Millipore) and an YM3 membrane (cutoff = 3 kDa). The concentrated solution (about 200 ml) was frozen dry and redissolved to 30 ml. The solution was then dialyzed against 5 × 1 L of ultrapure water (MilliQ).

The extract was filtered (0.45 μm) and then subjected to reverse-phase high-performance liquid chromatography (HPLC) on a C18 column (Prep Nova-Pak HR C18, Waters WAT025820, 7.8 × 300 mm) using a gradient of 0 to 100% acetonitrile at a flow rate of 0.8 ml/min for 70 min, monitoring at 280 nm. The collected fractions were analyzed via sodium dodecyl sulfate-polyacrylamide gel electrophoresis (SDS-PAGE) on 15% acrylamide gels. Mass spectra were measured on a matrix-assisted laser-desorption ionization-time-of-flight mass spectrometer (MALDI-TOF; Reflex III; Bruker, Billerica, MA). The protein concentration was determined via the BCA Protein Assay (Pierce) using bovine serum albumin (BSA) as a standard. Amino acid composition of the extract and the fractions were analyzed with a Hitachi 835-50 amino-acid analyzer (Japan) after lyophilized and hydrolyzed under 6 M HCl vapor in vacuum for 24 h.

Influence on Calcium Carbonate Precipitation. To create the saturated $CaCO_3$ solution, 20 mM $CaCl_2$ in 5 ml of 3 mM Tris (pH 8.7) was poured into 20 mM $NaHCO_3$ in 5 ml of 3 mM Tris (pH 8.7) at t = 0. The protein p10 (40 μg) was introduced in 80 μl of 3 mM Tris (pH 8.7). There was a sudden pH drop when we added the $CaCl_2$ into the hydrogen carbonate solution. This shift was quite reproducible and was recorded to determine calcium carbonate precipitation (Wheeler et al., 1981).

Crystallization Studies. The supersaturated crystallization solution was prepared by purging a stirred aqueous suspension of $CaCO_3$ with CO_2 (Samata et al., 1999). Crystallization experiments for scanning electron microscopy (SEM) and Raman spectroscopy were carried out by adding 3 μl of p10 (20 μg/ml) to 12 μl of supersaturated crystallization solution (20 μg/ml BSA or ultrapure water with same volume was used as control), which was dropped onto a glass cover slip situated at the bottom of a six-hole microplate and air-dried in a desiccator. The cover slips were gold coated and then observed in a Hitachi S-450 SEM.

Raman Microprobe Spectroscopy. To determine the polymorphisms of the crystals, the crystals were first observed with a Leica microscope (Germany) at a magnification of ×20 by using reflected white light. After focusing on the crystal, the light source of the microscope was transferred to a diode laser (514 nm). The sample was scanned for 10 s in the range 100 to 1500 cm^{-1} with a Renishaw RM1000 Raman imaging microscope (New Mills, UK). The Raman laser beam was then focused on the same crystal at the same location for two additional times.

X-Ray Diffraction of Crystals. The samples analyzed by X-ray diffraction were synthesized according to the method of Aizenberg et al. (1997). The crystals were grown by slow diffusion (about 3 days) of $(NH_4)_2CO_3$ vapor into six-hole microplate wells containing glass cover slips overlaid by 20 mM $CaCl_2$ (pH 7.0) solution without any protein or with 10 μg/ml of BSA or 10 μg/ml of p10 in a closed

desiccator. The glass coverslips covered with calcium carbonate crystals were rinsed with water and dried. The crystals were observed under a Leica DMIRB phase contrast and differential interference contrast microscope (Germany). The polymorphism of crystals was then determined by a D/max-RB X-ray diffractometer (Rigaku, Japan) with 40 keV Cu K_α radiation.

Cell Culture and Biological Assays of p10. The human fetal lung fibroblastic cell line MRC-5 and the mouse osteogenic cell line MC3T3-E1, were obtained from the cell conservation center of Peking Union Medical College Hospital (Beijing, China). MRC-5 cells were cultured in MEM (Gibco) supplemented with 10% heat-inactivated fetal bovine serum (FBS; Hyclone), 2 mM L-glutamine, and antibiotics (100 IU/ml of penicillin and 100 μg/ml of streptomycin). MC3T3-E1 cells were cultured in DMEM (Hyclone), supplemented with 10% heat-inactivated FBS and antibiotics. These two types of cells were both incubated at 37°C in 5% CO_2 humidified atmosphere and the media were changed every 3 days.

Two types of cells were plated out in 96-well plates at a density of 5×10^3 cells/well for 24 h and the agent to be test was added for 7 days. To measure the alkaline phosphatase (ALP) activity, the cells were washed with phosphate-buffered saline (PBS, pH 7.2) and then lysed with 0.1% Triton X-100 in 200 μl of 0.1 M $NaHCO_3$-$NaCO_3$ buffer (pH 10) with 2 mM $MgCl_2$ and 8 mM *p*-nitrophenol inorganic phosphate (pNPP) for 30 min. The absorbance at 405 nm was then measured by a Model 550 microplate reader (Bio-Rad). The total protein concentration of the lysates were determined by incubating the lysates (25 μl) with BCA protein assay reagents (Pierce) at 37°C for 30 min, then the absorbance at 550 nm was measured with the microplate reader. To determine the cell viability, cells were incubated with 0.5 mg/ml of MTT (3-(4,5-demethylthiazol-2-yl)-2,5-diphenyltetrazolium bromide) in the last 4 h of the culture period. The medium was then decanted, formazan salts were dissolved with 200 μl of dimethyl sulfoxide (DMSO), and the absorbance was determined at 490 nm in the microplate reader. Statistical analysis was performed using one-way analysis of variance (ANOVA) and the means were compared using Tukey's test.

Results

Purification and Characterization of p10. To preserve the bioactivities of the soluble matrix proteins, they were extracted from the nacre powder of *P. fucata* with a phosphate buffer (pH 7.0). The analysis of total extract by SDS-PAGE (Figure 1a, lane 3) showed that this extract was mainly composed of low molecular weight matrix proteins. A band of the major protein with apparent molecular mass of 10 kDa was also found in this extract. The total extract was then subjected to reverse-phase HPLC to purify this 10-kDa protein, and three main peaks appeared in the result (Figure 2). SDS-PAGE analysis (Figure 1a, lanes 2 and 5) showed that the last peak (peak 3) was a single protein with apparent molecular mass of 10 kDa, so we designated it as p10. The mass spectrum of p10 showed a single protonated ion peak at m/z 6813.82 (Figure 1b). The yield of p10 estimated by the BCA method was approximately 50 ng/g of nacre powder.

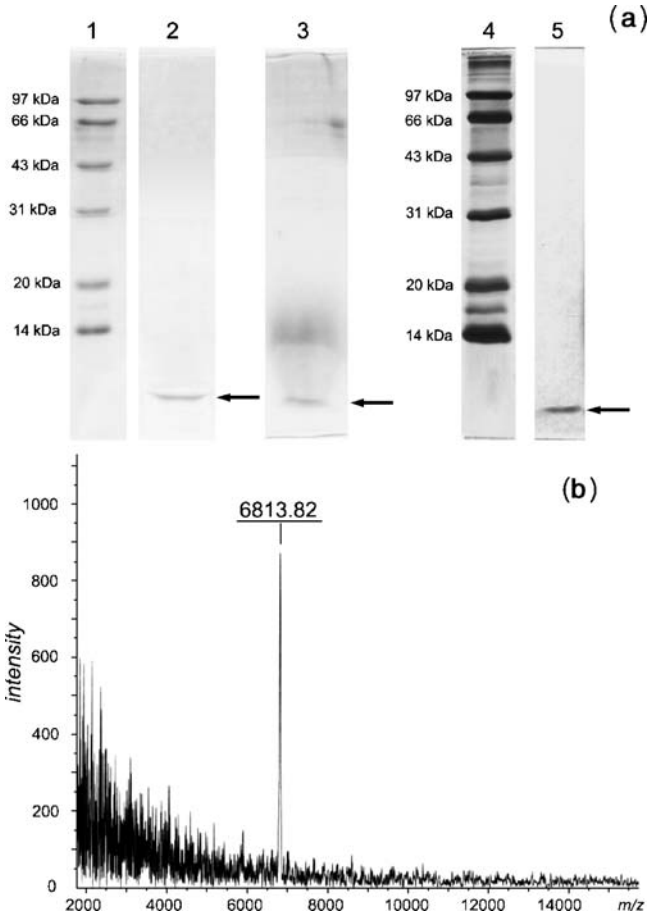

Fig. 1. (**a**) SDS-PAGE and (**b**) MALDI-TOF mass spectrometry of the purified protein p10 after reverse-phase HPLC. *Lanes 1* and *4*, molecular weight standards with masses indicated on the left. *Lanes 2* and *5*, purified p10 with a molecular mass of about 10 kDa (black arrow). *Lane 3*, protein band pattern of total extract, including p10 (black arrow). The gels containing lanes 1 to 3 were stained with Coomassie Brilliant Blue, while the gels containing lanes 4 and 5 were stained with silver salt.

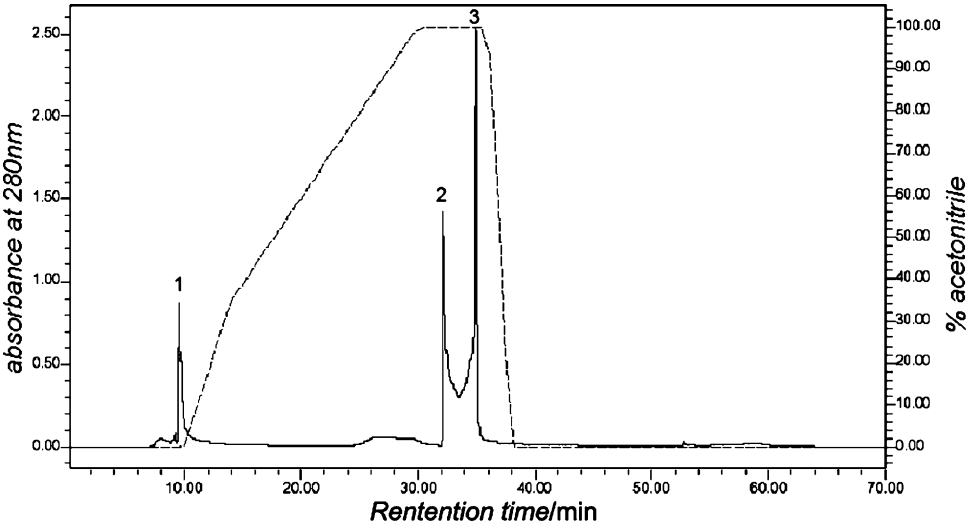

Fig. 2. Reverse-phase HPLC profile of the total extract. Samples of 100 μl were eluted with a gradient from 0% to 100% acetonitrile (dashed line) at a flow rate of 0.8 ml/min. Peak 3 (p10) was collected for further analysis.

The amino acid composition data of the total extract and p10 are shown in Table 1. In both samples, the contents of Gly, a predominant amino acid residue always found in nacre matrix, were the highest (nearly 40 mole%). The contents of Asx, an amino acid residue often found in soluble matrix extracted with EDTA or acid, were lower, especially in p10 (7.4%). In contrast, the leucine content of p10 (15.7%) was much higher than the total extract (7.5%). In addition, the p10 exhibited a charge to hydrophobic ratio (C/HP, Asx, Glx, His, Arg, Lys/Ala, Pro, Val, Met, Ile, Leu, Phe) of 0.42, and this ratio of the total extract is 0.76, indicating that our samples were all very hydrophobic (C/HP < 1).

Table 1. Amino Acid Compositions (Mole Percent) of the Total Extract and p10 of *Pinctada fucata*[a]

Amino acid	*Total extract*	*p10*
Asx	13.1	7.4
Thr	1.2	1.0
Ser	4.9	3.8
Glx	5.9	5.6
Gly	35.8	37.2
Ala	11.7	13.3
Val	3.2	2.0
Met	1.0	0.8
Ile	1.9	2.1
Leu	7.5	15.7
Tyr	3.4	2.6
Phe	2.8	3.5
Lys	1.8	1.5
His	0.4	0
Arg	2.5	1.8
Pro	2.9	1.7
C/HP[b]	0.76	0.42

[a]Cysteine, hydroxyproline, and tryptophan were absent in all samples. Hydroxylysine and phosphoserine were not determined.
[b]Ratio charged to hydrophobic residues (see the section on Influence of Calcium Carbonate Precipitation with p10 for details).

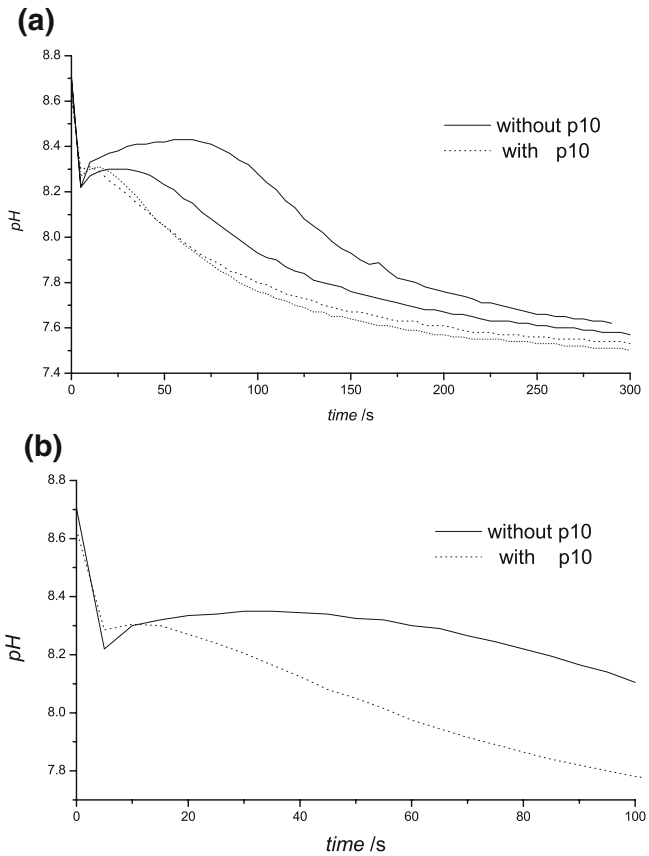

Fig. 3. Recordings of calcium carbonate precipitation in a saturated solution. (**a**) Effect of p10 on the precipitation of calcium carbonate. The pH of the solution was recorded as a function of time. (**b**) Averages of the data in (**a**) for the first 100 s of the pH measurements.

Influence of Calcium Carbonate Precipitation with p10. The effect of p10 on the rate of $CaCO_3$ precipitation was determined by recording the decrease of pH in a saturated calcium carbonate solution. The initial pH, which depends on calcium carbonate concentration, was chosen to be 8.7, where calcium carbonate precipitates at room temperature in less than 5 min. Recordings of a series of precipitation experiments with or without p10 (Figure 3) showed that the time course could be divided into the following stages. First, when $CaCl_2$ was added to $NaHCO_3$ to form the saturated solution, the pH dropped nearly instantly. This sudden shift might be due to the formation of a complex among the ionic species, which is different from nucleation. Second, there was a slight increase of the pH, followed by a relatively stable period for a few seconds. Finally, nucleation and precipitation occurred (Wheeler et al., 1981). With p10 in solution, the duration of the stable period was decreased compared with control, and the slope of the precipitation curve of calcium carbonate was also slightly steeper than the precipitation slope of control measurements in the first 100 s (Figure 3b). All these points suggested that p10 could accelerate the precipitation of calcium carbonate and it can be stated more surely that there is no inhibition on crystal growth by p10.

Morphology and Polymorph Determination of Calcium Carbonate Crystals Grown with p10. To investigate further the influence of p10 on calcium carbonate crystals, the morphology of crystals grown with p10 or BSA, or without any protein was observed via SEM (Figure 4). The crystals grown in the absence of p10 (both with BSA and without any protein) all exhibited the characteristic rhombohedral morphology of calcite (Figure 4a and b). However, crystals grown in the presence of p10 showed two kinds of morphologies different from each other (Figure 4c). Some of the crystals also exhibited the rhombohedral morphology of the calcite, while the other crystals grown with p10 displayed a cluster, needle-like morphology (Figure 4d), which is the conventional morphology of aragonite.

Two methods, Raman microprobe spectroscopy and X-ray diffraction, were employed to determine the polymorphs of the calcium carbonate crystals observed. The polymorphs of individual crystals with different morphology were analyzed in situ via Raman microscopy (Figure 5). The small needle-like crystals grown in the presence of p10 produced the characteristic Raman bands for aragonite at 206, 703, and 1085 cm^{-1} (Figure 5a), whereas the rhombohedral crystals in all samples exhibited the characteristic Raman bands for calcite at 282, 712, and

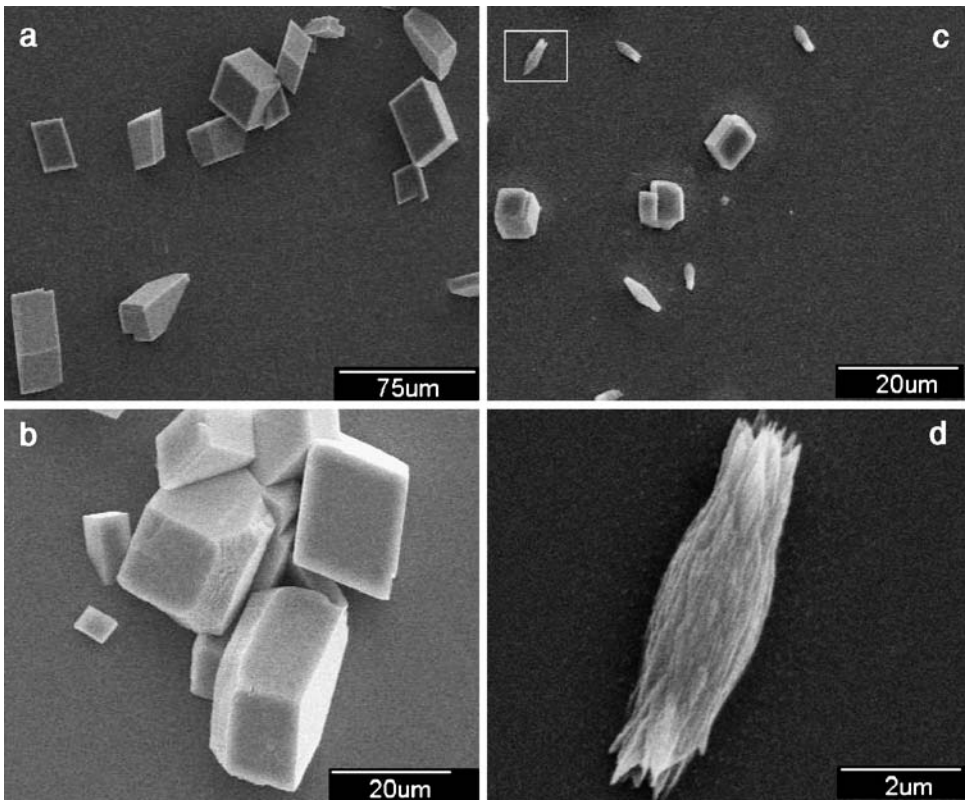

Fig. 4. SEM images of crystals grown in supersaturated calcium carbonate solution with (**a**) ultrapure water (control), (**b**) BSA (control), or (**c**) p10. (**d**) Enlarged image of the boxed part in (**c**).

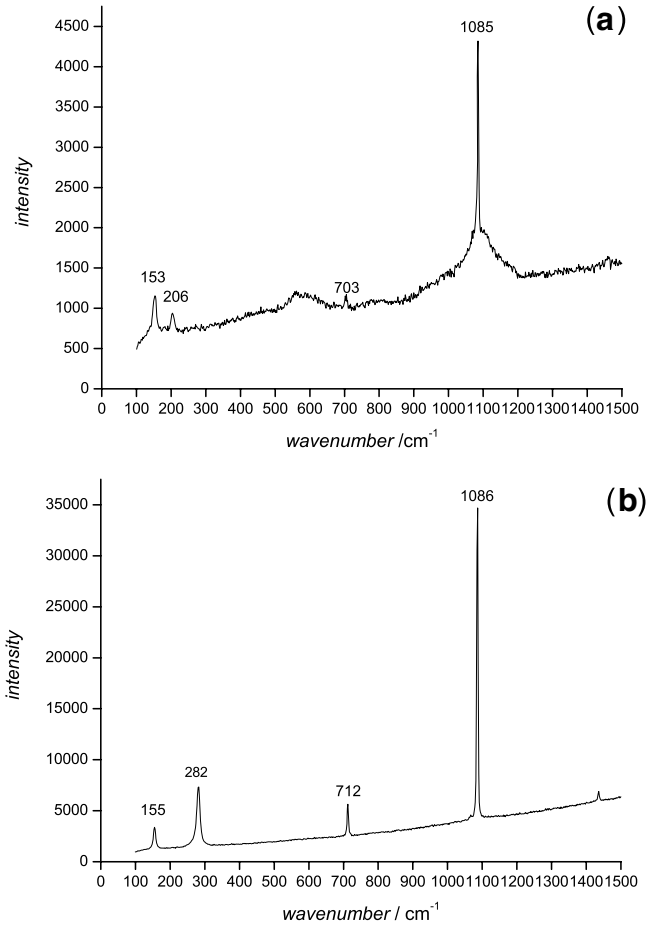

Fig. 5. Raman spectra of crystals with different morphology. (**a**) Raman spectrum of an individual needle-like aragonite crystal grown with p10 for polymorph determination. Characteristic Raman bands for aragonite are at 206, 703, and 1085 cm^{-1}. (**b**) Raman spectrum of an individual rhombohedral calcite crystal. Characteristic Raman bands for calcite are at 282, 712, and 1086 cm^{-1}.

1086 cm^{-1} (Figure 5b) (Fu et al., 2005). The X-ray diffraction patterns, an analysis of bulk crystal samples, are shown in Figure 6. The strongest diffraction intensity was the calcite (104) and the next-to-strongest was the calcite (208) for all the crystal samples, while the diffraction intensity of aragonite (022) could be seen only in the patterns with p10 (Figure 6c). It appeared that p10 induced the aragonite formation.

Effects of p10 on Cell Proliferation and Differentiation. As nacre matrix was thought to contain osteogenic signal molecules, two cell types, MRC-5 (a fibroblast cell line) and MC3T3-E1 (a preosteoblast cell line), which has the capacity to differentiate into osteoblasts, were employed to investigate the biological activity of the p10. ALP activity was measured to estimate the differentiation of the cells. ALP is expressed in the early stage of osteoblast development and is an accepted indicator of osteoblast differentiation. High ALP activity is generally considered as the first marker of osteoblast maturation (Quarles et al., 1992; Choi et al., 1996). The effects of p10 on ALP activity of both cell types were dose dependent (Figure 7a). The ALP activities

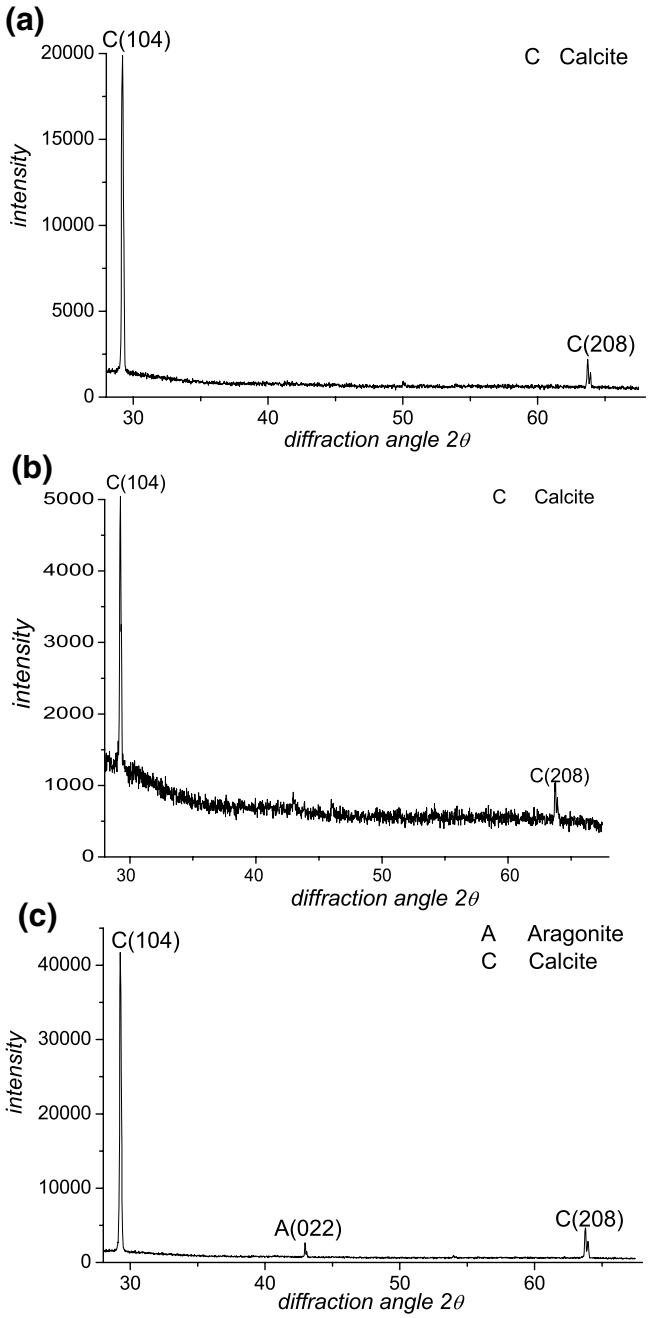

Fig. 6. X-ray diffraction pattern of the calcium carbonate crystals grown on a glass surface (**a**) without any protein, or with (**b**) BSA or (**c**) p10.

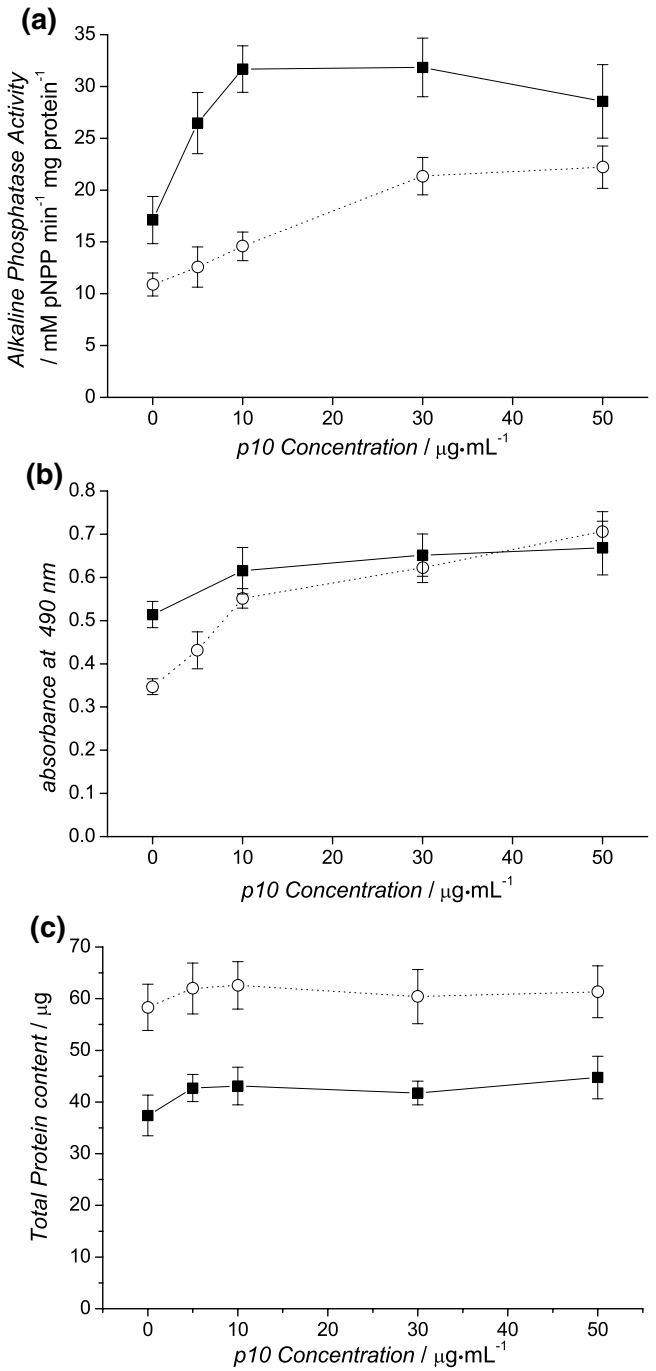

Fig. 7. Effect of p10 on (**a**) ALP activity, (**b**) MTT response, and (**c**) total protein content in MRC-5 cells (—■—) and MC3T3-E1 cells (····○····). Cells were treated with different concentrations of p10 for 7 days. Results are expressed as the mean ± SD for six wells.

of MRC-5 cells increase significantly ($p < 0.01$) at concentrations of 5 and 10 μg/ml of p10, and higher p10 concentrations (30 and 50 μg/ml) did not increase the ALP activity of MRC-5. The effects of p10 on the ALP activity of MC3T3-E1 cells were slightly different from those of MRC-5 cells. A concentration of 5 μg/ml of p10 had no significant effect on ALP activity increase ($p = 0.44$), whereas higher concentrations of p10 caused ALP activity increased significantly ($p < 0.01$) and the maximum effects were achieved at a concentration of 50 μg/ml. The increase of ALP activity of these two cell types implied that p10 could influence the differentiation process of fibroblasts and preosteoblasts in bone formation.

MTT assay, an enzymatic test based on quantification of activity of the mitochondrial dehydrogenase enzymes (Mosmann, 1983), was used to determine the effects of p10 on cell viability (Figure 7b). In both cell types, MTT response increased significantly ($p < 0.01$) with the concentrations of p10 changed, and achieved maximum effects at a concentration of 50 μg/ml of p10. It appeared that p10 could enhance the viability of these two types of cells. The MTT mitochondrial test provides a global measure of the number of viable cells and of their in vitro mitochondrial activity; cellular metabolic activation can thus be detected even in the absence of proliferation (Mosmann, 1983). To know whether the increase in the MTT response was the result of the activation of cell metabolism or to cell proliferation, we compared the results of MTT assay with the data of total protein content of ALP activity assay (Figure 7c). The total protein contents of both cell types and all concentrations of p10 were not significantly different from control ($p > 0.05$) except at 50 μg/ml of p10 in MRC-5 cells ($p = 0.008$), which appeared that the total protein content increased slightly in the present of p10. Thus this activation of MTT response would be attributed to the metabolism increase of viable cells but not to an increase in cell number. Therefore, we assumed that p10 does not act on the proliferation process but only on the differentiation process.

Discussion

The preservation of the integrity and activity of the macromolecules in nacre during the process of extraction is a difficult task. Previous studies only found that the soluble nacre matrix extracted by water without decalcification has the biological activity of inducing bone formation (Lamghari et al., 1999; Almeida et al., 2000, 2001; Moutahir-Belqasmi et al., 2001; Pereira-Mouries et al., 2002a; Rousseau et al., 2003; Lopez et al., 2004). We chose to use a phosphate buffer (pH 7.0) because it is more similar to the physiological condition of nacre-induced bone formation in vivo or in vitro. In accordance with previous studies, the soluble matrix extracted with EDTA was aspartate-rich and hydrophilic (C/HP > 1), while the

matrix extracted with water used to investigate biological activity was hydrophobic (C/HP < 1) (Weiner, 1979; Wheeler et al., 1988; Pereira-Mouries et al., 2002b). Amino acid composition analysis showed that the soluble matrix extracted with phosphate buffer (pH 7.0) was also very hydrophobic (C/HP < 1) and was not aspartate-rich, just similar to the soluble matrix extracted with water. Interestingly, this extract is composed mainly of the low molecular weight matrix proteins, which exhibited high bioactivity in previous studies (Almeida et al., 2000; Pereira-Mouries et al., 2002a). As initial separation by gel exclusion chromatography or ion-exchange chromatography did not achieve satisfactory results (data not shown), reverse-phase HPLC was used as the next isolation process. In the most hydrophobic fraction, we identified a novel protein, p10, which appears to play a significant role in nacre biomineralization.

Among the crystalline polymorphs of calcium carbonate, aragonite is thermodynamically less stable than calcite, and the calcium carbonate precipitated in abiotic condition is usually calcite. So it is of interest to know how the pearl oysters control the calcium carbonate precipitate as aragonite in the nacre and the pearls. Some researchers showed that insoluble matrix proteins may control the polymorphs of calcium carbonate crystals (Watabe and Wilbur, 1960; Wilbur and Watabe, 1963; Wheeler, 1992; Zhang and Zhang, 2006). In contrast, more evidence showed that the soluble matrix proteins play more important roles in polymorphic control (Weiner, 1979; Wheeler et al., 1988; Belcher et al., 1996; Falini et al., 1996; Zaremba et al., 1996; Feng et al., 2000; Thompson et al., 2000; Zhang and Zhang, 2006). Besides these studies, some purified proteins such as the N16 family, pearlin, perlucin, N14, and N66 also exhibited the ability to influence the polymorphs of calcium carbonate, but they induced the formation of aragonite crystals only when associated with other matrix proteins or insoluble organic matrix (Samata et al., 1999; Kono et al., 2000; Matsushiro et al., 2003; Blank et al., 2003). Different from them, p10 could direct the calcium carbonate crystal polymorphism by itself. Further, that p10 could accelerate the precipitation of calcium carbonate, just as perlucin (Weiss et al., 2000), implied that the effects of p10 are mainly in the nucleation regime. This result was different from the previous results of soluble matrix extracted with acetic acid or EDTA (Wheeler et al., 1981; Marin et al., 2000), which inhibited the precipitation of calcium carbonate and was thought to modify crystal growth. These suggested that p10 might control the polymorphs of calcium carbonate crystal by making the calcium carbonate nucleate directly as aragonite. As p10 provide nucleation sites for the calcium carbonate in this hypothesis, it could accelerate the precipitation speed in the calcium carbonate precipitation experiments. Surprisingly, p10 did not exhibit Ca^{2+} binding capability (data not shown); therefore, the polymorphic control mechanism of p10 may not involve in Ca^{2+} binding, but seems to be related to the modulating the stereochemical position of CO_3^{2-} in the crystal lattice. However, besides aragonite, calcite also existed in the crystals grown with p10. It seems that the effect of p10 is only to make the calcium carbonate form as aragonite, but it could not change the formed calcite into aragonite. As there also existed other nucleation sites besides p10 in the system of crystal growth, the thermodynamically stable calcite could also form and could not be changed into aragonite.

Matrix proteins appear not only to control the crystal formation of the shell, but also to affect the cells participating in the biomineralization. The nacre soluble matrix extracted with water can induce the proliferation and differentiation of cultured bone-related cells (Lamghari et al., 1999; Almeida et al., 2000, 2001; Moutahir-Belqasmi et al., 2001; Pereira-Mouries et al., 2002a; Rousseau et al., 2003; Lopez et al., 2004). They also exhibited similar effects on primitive cultured abalone mantle cells (Sud et al., 2001). However, until now no matrix protein isolated from the soluble matrix extracted with water has been reported, although this extract was thought to contain osteogenic signals molecules. On the other hand, some shell matrix proteins identified, such as perlustrin of *Haliotis laevigate* (Weiss et al., 2001) and dermatopontin of *Biomphalaria glabrata* (Marxen et al., 2003), were speculated to have effects on the mineralogenic cells according to sequence similarity, but these effects were not proven by experiments. The p10, extracted also via a undecalcifying process, was able to enhance the MTT and ALP activity of MRC-5 fibroblasts, partially the same as did the soluble matrix extracted with water (Lamghari et al., 1999 ; Almeida et al., 2000, 2001; Moutahir-Belqasmi et al., 2001; Pereira-Mouries et al., 2002a). Different from the whole soluble matrix extracted with water (Almeida et al., 2000, 2001; Moutahir-Belqasmi et al., 2001; Pereira-Mouries et al., 2002a), p10 did not change the total protein content, suggesting that p10 would not influence the cell proliferation. All this evidence implies that p10 is an osteogenic factor in the nacre matrix.

In summary, p10, a novel matrix protein identified from the nacreous layer of pearl oyster, *Pinctada fucata*, plays important roles in controlling both calcium carbonate crystal formation and the

differentiation of cells participating in the biomineralization. The same phenomenon was also observed in mammals. Dentin matrix protein-1 (DMP-1), a matrix protein in mammalian bone and teeth, not only acted as a transcriptional regulator for activation of osteoblast-specific genes in the nucleus, but also regulated nucleation of hydroxyapatite when it was phosphorylated and exported to extracellular matrix (Narayanan et al., 2003). This similarity corroborates a previous hypothesis that phylogenetically distant (i.e., mollusc vs. mammal) biomineralization systems such as nacre and bone (teeth) are assembled at least in part from biochemical components inherited from common uncalcified ancestors (Westbroek and Marin, 1998). However, more characteristics, especially sequence information, are required to ascertain our speculation and elucidate how p10 directs the calcium carbonate crystal polymorph and induces cell differentiation.

Acknowledgments

This work was financially supported by the National High Technology Research and Development Program of China (2001AA621140), and the National Natural Science Foundation of China (30170723).

References

Aizenberg J, Hanson J, Koetzle TF, Weiner S, Addadi L (1997) Control of macromolecule distribution within synthetic and biogenic single calcite crystals. J Am Chem Soc 119, 881–886

Almeida MJ, Milet C, Peduzzi J, Pereira-Mouries L, Haigle J, Barthelemy M, Lopez E (2000) Effect of water-soluble matrix fraction extracted from the nacre of *Pinctada maxima* on the alkaline phosphatase activity of cultured fibroblasts. J Exp Zool 288, 327–334

Almeida MJ, Pereira L, Milet C, Haigle J, Barbosa M, Lopez E (2001) Comparative effects of nacre water-soluble matrix and dexamethasone on the alkaline phosphatase activity of MRC-5 fibroblasts. J Biomed Mater Res 57, 306–312

Atlan G, Delattre O, Berland S, LeFaou A, Nabias G, Cot D, Lopez E (1999) Interface between bone and nacre implants in sheep. Biomaterials 20, 1017–1022

Belcher AM, Wu XH, Christensen RJ, Hansma PK, Stucky GD, Morse DE (1996) Control of crystal phase switching and orientation by soluble mollusc-shell proteins. Nature 381, 56–58

Blank S, Arnoldi M, Khoshnavaz S, Treccani L, Kuntz M, Mann K, Grathwohl G, Fritz M (2003) The nacre protein perlucin nucleates growth of calcium carbonate crystals. J Microsc 212, 280–291

Choi JY, Lee BH, Song KB, Park RW, Kim IS, Sohn KY, Jo JS, Ryoo HM (1996) Expression patterns of bone-related proteins during osteoblastic differentiation in MC3T3-E1 cells. J Cell Biochem 61, 609–618

Falini G, Albeck S, Weiner S, Addadi L (1996) Control of aragonite or calcite polymorphism by mollusk shell macromolecules. Science 271, 67–69

Feng QL, Pu G, Pei Y, Cui FZ, Li HD, Kim TN (2000) Polymorph and morphology of calcium carbonate crystals induced by proteins extracted from mollusk shell. J Cryst Growth 216, 459–465

Fu G, Valiyaveettil S, Wopenka B, Morse DE (2005) $CaCO_3$ Biomineralization: acidic 8-kDa proteins isolated from aragonitic abalone shell nacre can specifically modify calcite crystal morphology. Biomacromolecules 6, 1289–1298

Jolly C, Berland S, Milet C, Borzeix S, Lopez E, Doumenc D (2004) Zona localization of shell matrix proteins in mantle of *Haliotis tuberculata* (Mollusca, Gastropoda). Mar Biotechnol 6, 541–551

Kamat S, Su X, Ballarini R, Heuer AH (2000) Structural basis for the fracture toughness of the shell of the conch *Strombus gigas.* Nature 405, 1036–1040

Kono M, Hayashi N, Samata T (2000) Molecular mechanism of the nacreous layer formation in *Pinctada maxima*. Biochem Biophys Res Commun 269, 213–218

Lamghari M, Almeida MJ, Berland S, Huet H, Laurent A, Milet C, Lopez E (1999) Stimulation of bone marrow cells and bone formation by nacre: in vivo and in vitro studies. Bone 25S, 91S–94S

Lamghari M, Berland S, Laurent A, Huet H, Lopez E (2001) Bone reactions to nacre injected percutaneously into the vertebrae of sheep. Biomaterials 22, 555–562

Lopez E, Vidal B, Berland S, Camprasse S, Camprasse G, Silve C (1992) Demonstration of the capacity of nacre to induce bone formation by human osteoblasts maintained in vitro. Tissue Cell 24, 667–679

Lopez E, Milet C, Lamghari M, Pereira-Mouries L, Borzeix S, Berland S (2004) The dualism of nacre. Key Eng Mater 254, 733–736

Marin F, Corstjens P, de Gaulejac B, de Vrind-De Jong E, Westbroek P (2000) Mucins and molluscan calcification: Molecular characterization of mucoperlin, a novel mucin-like protein from the nacreous shell layer of the fan mussel *Pinna nobilis* (Bivalvia, Pteriomorphia). J Biol Chem 275, 20667–20675

Marxen JC, Nimtz M, Becker W, Mann K (2003) The major soluble 19.6-kDa protein of the organic shell matrix of the freshwater snail *Biomphalaria glabrata* is an N-glycosylated dermatopontin. Biochim Biophys Acta 1650, 92–98

Matsushiro A, Miyashita T, Miyamoto H, Morimoto K, Tonomura B, Tanaka A, Sato K (2003) Presence of protein complex is prerequisite for aragonite crystallization in the nacreous layer. Mar Biotechnol 5, 37–44

Mosmann TJ (1983) Rapid colorimetric assay for cellular growth and survival: Application to proliferation and cytotoxicity assays. J Immunol Methods 65, 55–63

Moutahir-Belqasmi F, Balmain N, Lieberrher M, Borzeix S, Berland S, Barthelemy M, Peduzzi J, Milet C, Lopez E (2001) Effect of water soluble extract of nacre (*Pinctada maxima*) on alkaline phosphatase activity and Bcl-2

expression in primary cultured osteoblasts from neonatal rat calvaria. J Mater Sci Mater Med 12, 1–6

Narayanan K, Ramachandran A, Hao J, He G, Park KW, Cho M, George A (2003) Dual functional roles of dentin matrix protein 1: Implications in biomineralization and gene transcription by activation of intracellular Ca^{2+} store. J Biol Chem 278, 17500–17508

Pereira-Mouries L, Almeida MJ, Milet C, Berland S, Lopez E (2002a) Bioactivity of nacre water-soluble organic matrix from the bivalve mollusk *Pinctada maxima* in three mammalian cell types: Fibroblasts, bone marrow stromal cells and osteoblasts. Comp Biochem Physiol B 132, 217–229

Pereira-Mouries L, Almeida MJ, Ribeiro C, Peduzzi J, Barthelemy M, Milet C, Lopez E (2002b) Soluble silk-like organic matrix in the nacreous layer of the bivalve *Pinctada maxima*. Eur J Biochem 269, 4994–5003

Quarles LD, Yohay DA, Lever LW, Caton R, Wenstrup RJ (1992) Distinct proliferative and differentiated stages of murine MC3T3-E1 cells in culture: An in vitro model of osteoblast development. J Bone Miner Res 7, 683–692

Rousseau M, Pereira-Mouries L, Almeida MJ, Milet C, Lopez E (2003) The water-soluble matrix fraction from the nacre of *Pinctada maxima* produces earlier mineralization of MC3T3-E1 mouse pre-osteoblasts. Comp Biochem Physiol B 135, 1–7

Rubner M (2003) Materials science: Synthetic sea shell. Nature 423, 925–926

Samata T, Hayashi N, Kono M, Hasegawa K, Horita C, Akera S (1999) A new matrix protein family related to the nacreous layer formation of *Pinctada fucata*. FEBS Lett 462, 225–229

Silve C, Lopez E, Vidal B, Smith DC, Camprasse S, Camprasse G, Couly G (1992) Nacre initiates biomineralization by human osteoblasts maintained in vitro. Calcif Tissue Int 51, 363–369

Sud D, Doumenc D, Lopez E, Milet C (2001) Role of water-soluble matrix fraction, extracted from the nacre of *Pinctada maxima*, in the regulation of cell activity in abalone mantle cell culture (*Haliotis tuberculata*). Tissue Cell 33, 154–160

Takeuchi T, Endo K (2006) Biphasic and dually coordinated expression of the genes encoding major shell matrix proteins in the pearl oyster *Pinctada fucata*. Mar Biotechnol 8, 52–61

Thompson JB, Paloczi GT, Kindt JH, Michenfelder M, Smith BL, Stucky G, Morse DE, Hansma PK (2000) Direct observation of the transition from calcite to aragonite growth as induced by abalone shell proteins. Biophys J 79, 3307–3312

Watabe N, Wilbur KM (1960) Influence of the organic matrix on crystal type in mollusks. Nature 188, 334

Weiner S (1979) Aspartic acid-rich proteins: major components of the soluble organic matrix of mollusk shell. Calcif Tissue Int 29, 163–167

Weiss IM, Kaufmann S, Mann K, Fritz M (2000) Purification and characterization of perlucin and perlustrin, two new proteins from the shell of the mollusk *Haliotis laevigata*. Biochem Biophys Res Commun 267, 17–21

Weiss IM, Gohring W, Fritz M, Mann K (2001) Perlustrin, a *Haliotis laevigata* (abalone) nacre protein, is homologous to the insulin-like growth factor binding protein N-terminal module of vertebrates. Biochem Biophys Res Commun 285, 244–249

Westbroek P, Marin F, (1998) A marriage of bone and nacre. Nature 392, 861–862

Wheeler AP (1992) "Phosphoproteins of oyster (*Crassostrea virginica*) shell organic matrix." In: *Hard Tissue Mineralization and Demineralization*, Suga S, Watabe N, eds. (Tokyo/New York: Springer-Verlag) pp 171–187

Wheeler AP, George JW, Evans CA (1981) Control of calcium carbonate nucleation and crystal growth by soluble matrix of oyster shell. Science 212, 1397–1398

Wheeler AP, Rusenko KW, Swift DM, Sikes CS (1988) Regulation of in vitro and in vivo $CaCO_3$ crystallization by fractions of oyster shell organic matrix. Mar Biol 98, 71–80

Wilbur KM, Watabe N (1963) Experimental studies on calcification in mollusks and the alga *Cocolithus huxleyi*. Ann NY Acad Sci 109, 82–112

Zaremba CM, Belcher AM, Fritz M, Li Y, Mann S, Hansma PK, Morse DE, Speck JS, Stucky GD (1996) Critical transitions in the biofabrication of abalone shells and flat pearls. Chem Mater 8, 679–690

Zhang C, Zhang R (2006) Matrix proteins in the outer shells of molluscs. Mar Biotechnol, in press

Zhang Y, Xie L, Meng Q, Jiang T, Pu R, Chen L, Zhang R (2003) A novel matrix protein participating in the nacre framework formation of pearl oyster, *Pinctada fucata.* Comp Biochem Physiol B 135, 565–573